



RESEARCH ARTICLE

Computational screening for the identification of potent tubulin inhibitors as anticancer agents

Priyanka Sharma, Vivek Asati

Department of Pharmaceutical Chemistry, ISF College of Pharmacy, Moga, Punjab, India

ABSTRACT

Tubulin is a biological target for several multiple clinically used anticancer drugs which is responsible for chromosome segregation, cell shape maintenance, transport, motility, and organelle dispersion, among other things. For decades, anticancer medicines that target the microtubule, such as taxanes and vinca alkaloids, have formed the cornerstone of many chemotherapy regimens. However, these medicines have substantial drawbacks, prompting the development of new microtubule targeting compounds. The pyrazole ring system is a critical component of various tubulin inhibitors discovered in recent years. In the present study, a dataset of tubulin inhibitors have been downloaded from PubMed database and included for screening study by Glide module. The Lipinski rule of 5, high-throughput virtual screening, standard precision, and extra precision methodologies have been used for final screening of potent compounds against tubulin protein (PDB ID: 3E22). The docking studies of these inhibitors revealed a complementary fit in the allosteric site of Tubulin protein. Among all the selected inhibitors, Centaureldin and Chalcones MDL showed the highest docking scores of -7.76 and -6.21 kcal/mol, respectively, when compared with the cocrystal ligands of PDB-3E22. Post-molecular mechanics/generalized born surface area analysis of these potent inhibitors showed dG binding values -37.83 and -28.37 kcal/mol, respectively. On the basis of final screened compounds, we can further develop pharmacophore model and screened potential compounds against tubulin protein.

KEY WORDS: Extra precision, High throughput virtual screen, Pharmacophore model, Standard precision, Tubulin inhibitors, Virtual screening

INTRODUCTION

Tubulin is a biological target for several multiple clinically used anticancer drugs which is responsible for chromosome segregation, cell shape maintenance, transport, motility, and organelle dispersion, among other things.^[1] For decades, anticancer medicines that target the microtubule, such as taxanes and vinca alkaloids,^[2] have formed the cornerstone of many chemotherapy regimens. Drugs targeting microtubular proteins are a significant and promising anticancer therapeutic class, including antimetabolic and antiangiogenic^[3] characteristics in addition to slowing tumor growth in cancer and endothelial cells [Figure 1]. Colchicine binding site (CBS) is one of five significant known binding sites on tubulin protein^[4] with

the longest history of anticancer research. However, these medicines have substantial drawbacks, prompting the development of new microtubule targeting compounds.^[5] The pyrazole ring system is a critical component of various tubulin inhibitors discovered in recent years.^[6] Cancer deaths are increasing dramatically, and it will be the leading cause of death in all age groups by 2020.^[7] As a result, there is a significant global demand for rapidly approved and effective anticancer drug candidates.^[8] Due to breakthrough improvements in the fields of molecular, genomic, and phenotypic data of pharmacological drugs, computational

Address for Correspondence:

Vivek Asati,

E-mail: vivekasatipharma47@gmail.com

Access this article online

Website:

<http://isfcpsharmaspire.com>

DOI:

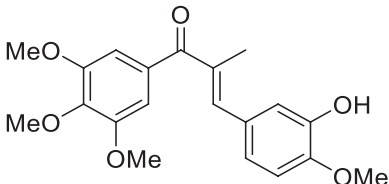
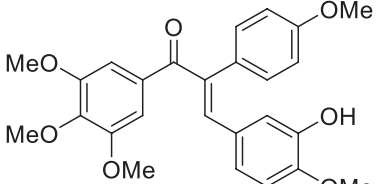
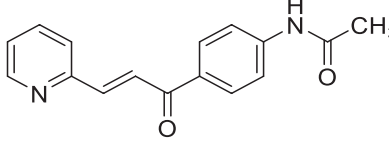
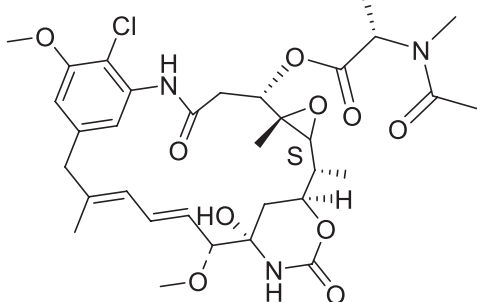
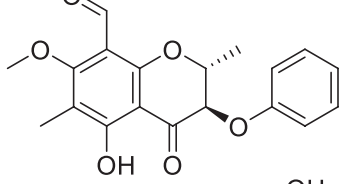
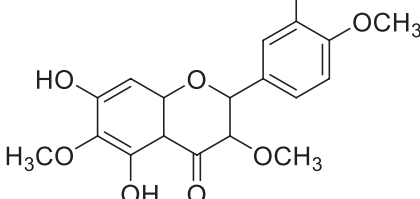
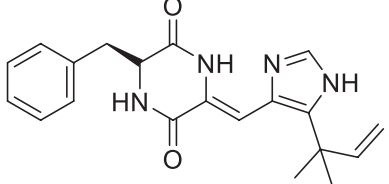
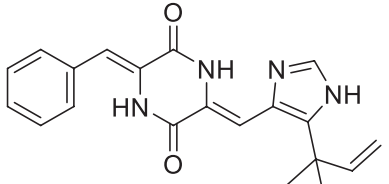
10.56933/Pharmaspire.2022.14209

Date of Submission: 07 July 2022

Date of Revision: 14 July 2022

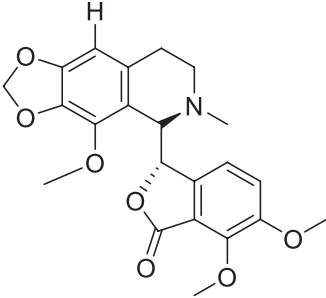
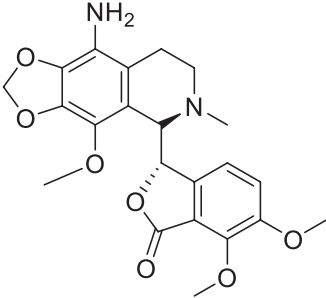
Date of Acceptance: 19 July 2022

Table 1: The compounds were used for the screening of the potential tubulin inhibitors

S. No.	Compound name	Structures	Database Coding
1	Chalcone SD400		10451021
2	Alpha-arylchalcone		46224385
3	Chalcone MDL		16970393
4	Maytansine		10274768
5	Desmosdumotin A		16737621
6	Centaureidin		5315773
7	(-)- phenylahistin		9798496
8	(Z)-Dehydrophenylahistin		9902905

(Contd...)

Table 1: (Continued)

S. No.	Compound name	Structures	Database Coding
9	Noscapine		275196
10	Amino-noscapine		46175165

drug repurposing, a new area of drug repurposing, has been aggressively developed. Drug repurposing is an expedited strategy for chemical development that involves looking for new indications^[9] for already approved treatments rather than exploring *de novo* drug compounds from scratch, and it now accounts for 30% of newly approved drugs in the United States.

SOFTWARES AND METHODOLOGIES

Selection of data set

Ten molecules have been selected which have Tubulin inhibitory activity [Table 1]. The datasheet structures were sketched using ChemDraw professional 16.0 and mol format (.mol)^[10] was used to store. Optimization of various performance structures helps in understanding the various requirements of simulation models and is found very useful. To convert 2D structures into 3D structures quickly, a Clean-up wizard was used which can convert one ligand per second.^[11] The use of optimization algorithms was very helpful in the production of pharmacophore and docking studies depicts various molecules which have been arranged in a manner on a common scaffold after energy minimization.^[12]

Ligand preparation for docking

Ligprep from the Schrödinger suite was used to prepare the ligands. The first ligand databases were obtained as collections of SMILES^[13] (simplified molecular input line-entry system) strings (without 3D coordinates). The energy was then decreased using the Optimized Potentials for Liquid Simulations (OPLS2005) force field in the Ligprep

module of the software,^[14] and ligands were included into the workstation (Schrodinger). This minimization aids in bond order assignment, ligand hydrogen addition, and the conversion of 2D to 3D structure for docking experiments.^[15] The best conformations of the ligands output file were then used for docking investigations (Schrodinger release).

Protein preparation with protein preparation wizard

The Protein Preparation Wizard in the Schrödinger suite was used to process the PDB protein ligand structures.^[16] Using Prime, missing residues and loop segments near the active site were added, and the protein structure integrity was evaluated and modified.^[17] Following the deletion of any original hydrogen atoms, bond ordering for amino acid residues and the ligand was adjusted. Asp, Glu, Arg, Lys, and his protonation and tautomeric states were altered to match a pH of 7.4. Possible Asn and Gln residue orientations were produced. Water molecules at the active site of the ligand that were beyond 5.0 were removed. Non-water water molecules with fewer than two hydrogen bonds were removed. The protein ligand complex was then refined geometrically using an OPLS2005 force field restrained minimization with heavy atom convergence to an RMSD of 0.3.^[18]

Molecular docking

Computational tools are critical in the drug design process, particularly to take advantage of the growing number of solved X-ray and NMR proteinligand structures.^[19] Molecular docking methods are nowadays used to predict protein-ligand interactions and to aid in the selection

of potent molecules as part of virtual screening of large databases.^[20] The advances in computational capacity over the past decade have enabled further developments in molecular docking algorithms to address more complicated aspects such as protein flexibility. Protein-ligand docking is an effective tool for studying and comprehending protein-ligand interactions.^[21] Docking is frequently used in drug design strategies at various stages, such as to make the design of potentially active leads easier. Finding the best ligand poses and properly ranking the relative docking propensity of several ligands are critical.^[22] In practice, molecular docking requires three structural data sets for candidate ligands and the protein target of interest,^[23] as well as a procedure for estimating protein-ligand interaction poses and strengths. Protein target structures for docking studies are primarily obtained from the RSCB Protein Data Bank (PDB) repository.^[24] For many years, the number of structures deposited in the PDB repository has been rapidly increasing.

Protein ligand sampling algorithms are required by docking software applications in order to generate acceptable ligand poses. Docking algorithms may treat the protein as a stiff body, a soft body, with flexible side chains, or with specific flexible domains. Protein flexibility can also be represented by several conformers or ensembles of stiff protein structures.^[25] To assess the binding affinities of ligand poses, many kinds of scoring functions are applied. Force field-based, empirical, knowledge-based, clustering and entropy-based, or consensus scoring methods are the various types of scoring functions.^[26]

Molecular mechanics/generalized born surface area (MM/GBSA) based rescoring

The free binding energies of the protein and ligand complexes were investigated using the MM-GBSA^[27] (molecular mechanics, the generalized born model, and solvent accessibility) approach. The ideal binding energy of the selected complexes with the lowest docking score was calculated using the prime module of Schrodinger program Package. The VSGB 2.0 model was used for the investigation, with an implicit solvent model and physics-based modifications for π - π interactions, hydrophobic interactions, and hydrogen bonding self-contact interactions.^[28]

In silico predicted physicochemical parameters: ADME property predictions

The physicochemical properties of the acquired hits after docking investigations were predicted *in silico* using Schrodinger's Qikprop module.^[29] The following parameters were predicted: Molecular weight (M.Wt.), number of hydrogen bond donors, number of hydrogen bond acceptors, octanol/water partition coefficient (log P), predicted apparent Caco-2 cell permeability in nm/sec

(P Caco), and number of rotatable bonds (Rot) (QikProp De Schrodinger Release).^[30]

RESULTS AND DISCUSSION

Docking

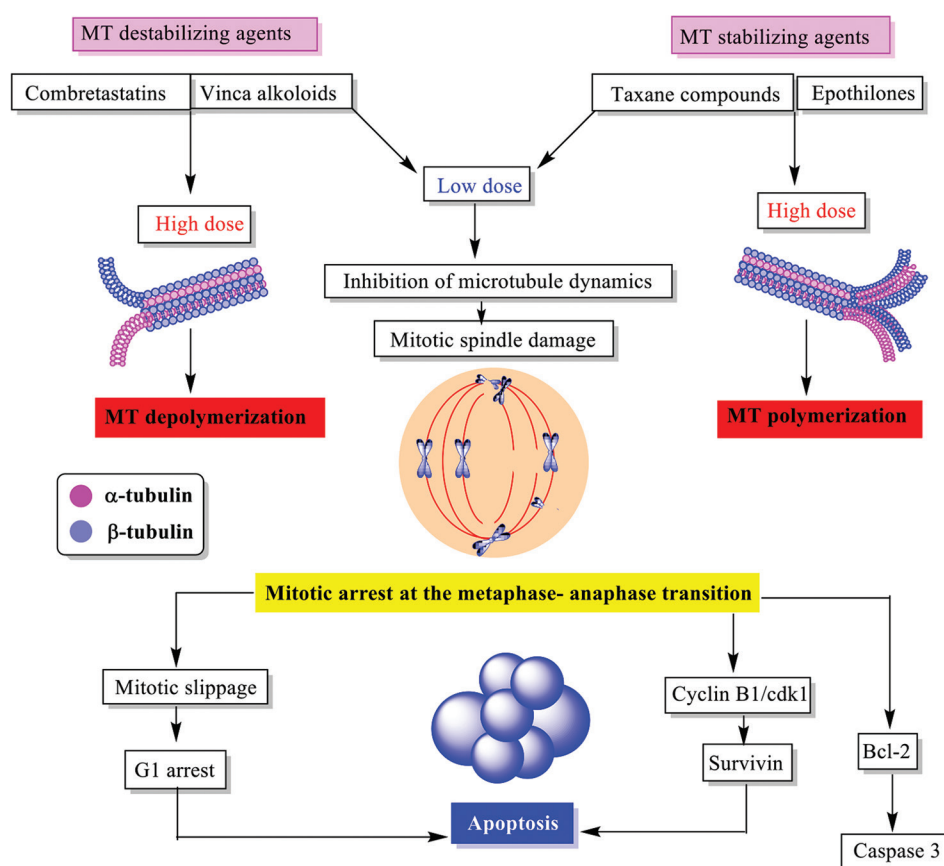
Molecular modeling studies were performed on Glide v5.8 (Schrodinger, LLC, New York, NY)^[31] to investigate the potential interactions between target compound and Tubulin-Colchicin-Soblidotin (PDB Code: 3E22). All the compounds were docked to various active sites of Tubulin-colchicine-soblidotin for studying the essential interactions of compounds with protein to produce anti-cancer activity.^[32] The docking studies were performed using Glide in the allosteric site of protein Tubulin-colchicine-soblidotin (PDB entry: 3E22) and validated by docking of 3E22 ligand in the allosteric site. The designed Tubulin-Colchicin inhibitors were docked in the allosteric binding site comprising of SER140, MG 601, GLU 71, ASN 101, ALA 12, THR 179, ASN 206, TYR 224, GLN 15, THR 145, MG 60, and residues. Table 2 showed the glide score by standard precision (SP) and extra precision (XP) and glide energy of the inhibitors. The docking studies of these inhibitors suggested a complementary fit in the allosteric site of the Protein (PDB ID: 3E22).

All the selected inhibitors were allowed to bind with the receptor as shown by the crystal ligand. The compound Centaureidin showed the best inhibitory activity with highest docking score of -7.762 [Figure 2], and showing the H-bond interactions with the amino acid residue of ASN206 (2.17), TYR224 (4.17), and GLY142 (2.77) represented by magenta arrow with the OH of benzene ring, and showing π - π stacking with the amino acid residue of TYR224 (4.17) and metal coordination with MG601 (1.96). In Figure 3, (Chalcone MDL), showed docking interaction in which the green line showed π - π stacking with the amino acid residue of TYR224 (3.91), and showing H bond interaction with GLN11 (2.34), and metal coordination with MG601 (2.10). Furthermore, Figure 4, compound Noscapine, in which the magenta arrow represents the H-bond interactions with the amino acid residue of ALA12 (2.65), and showing metal coordination with MG601 (2.15) and MG601 (2.23) with both oxygen atom attached to the benzene ring. Figure 5, compound (Z)-Dehydrophenylahistin, showed docking interaction in which the magenta arrow represents the H-bond interactions with the amino acid residue of SER140 (2.00), ASN 101(2.04), ALA12 (2.43) to the oxygen atom of the piperazine moiety, while GLU 71 (1.94) showing H-bond interactions with NH of pyrazole ring, and showing the metal coordination interaction in black with residue of MG 601 (2.05). In Figure 6, compound (-)-phenylahistin, the magenta arrow represents the H-bond interactions with the oxygen atom of piperazine dionemoeity the amino acid residue of SER140 (1.90), ASN 101(1.90), ALA12 (2.24),

Table 2: Docking scores (using HTVS, SP, and XP methodologies) with binding energy (using MMGBSA) of potent compounds

S. No.	Compound	Docking score (xp) kcal/mol	Docking score (sp) kcal/mol	MMGBSA dG bind (xp complex) kcal/mol
1	Centaureidin	-7.762	-7.553	-52.2812
2	Chalcones MDL	-6.211	-7.436	-31.5634
3	Noscapine	-5.518	-7.649	-
4	(Z)-Dehydrophenylahistin	-4.794	-7.186	-
5	(-)-phenylahistin	-1.829	-7.084	-1213.66
6	Desmosdumotin A	-	-7.08	-
7	Amino-noscapine	-	-7.045	-
8	Chalcone SD400	-	-7.028	-
9	Alpha-arylchalcone	-	-7.028	-
10	Mayatansine	-	-6.832	-

HTVS: High-throughput virtual screening, SP: Standard precision, XP: Extra precision

**Figure 1:** Polymerization of microtubules.

GLU 71 (2.14)-NH of pyrazole, and showing the metal coordination interaction in black with residue of MG 601 (2.00). Figure 7, in Compound Desmosdumotin A, the magenta arrow represents the H-bond interactions with the amino acid residue of GLN11 (2.22), THR145 (2.09), showing π - π stacking with the amino acid residue of TYR224 (4.32), and metal coordination with MG601 (2.07) and MG601 (2.09). Figure 8, Compound amino-Noscapine,

in which the magenta arrow represents the H-bond interactions with the amino acid residue of ALA12 (2.64), SER140 (1.89), ASN206 (1.84), and GLY146 (2.67), and showing metal coordination with MG601 (2.00) and MG601 (2.041). In Figure 9, Compound Chalcone SD400, the magenta arrow represents the H-bond interactions with the amino acid residue of GLN15 (2.09), GLY146 (2.74), THR145 (2.57), and showing π - π stacking with the amino

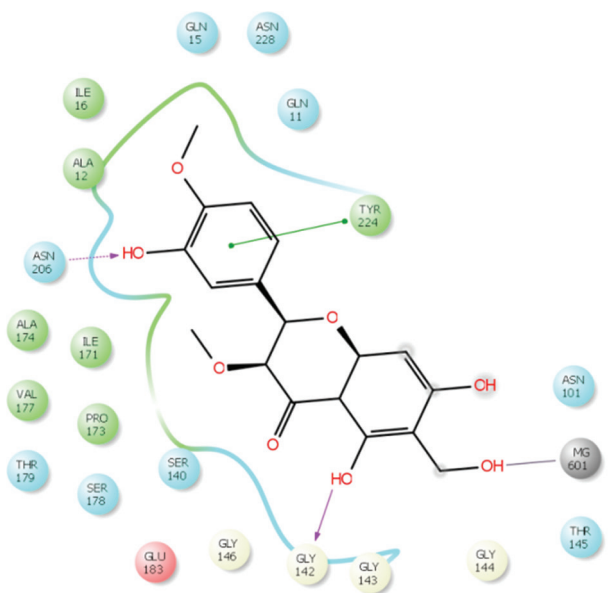


Figure 2: Amino-acid residue interactions exhibited by the molecule Centaureidin in the active site of the target PDB-3E22.

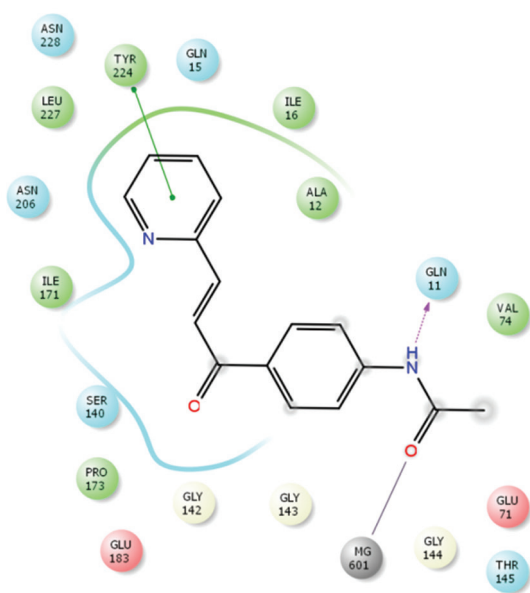


Figure 3: Amino-acid residue interactions exhibited by the molecule Chalcone MDL in the active site of the target PDB-3E22.

acid residue of TYR224 (3.99) and metal coordination with MG601 (2.05). Figure 10, Alpha-arylchalcone, in which the magenta arrow represents the H-bond interactions with the amino acid residue of SER140 (2.65), ASN 206 (1.86) and ASN101 (2.64), THR179 (1.82) and showing the metal coordination interaction in black with residue of MG601 (2.00). In Figure 11, compound Mayatansine, in which the magenta arrow represents the H-bond interactions with the amino acid residue of ASP98 (1.84) with the OH of Oxazine and ASP98 (2.05), ASN101 (2.168) with that of Oxygen atom, and showing metal coordination with MG601 (2.14).

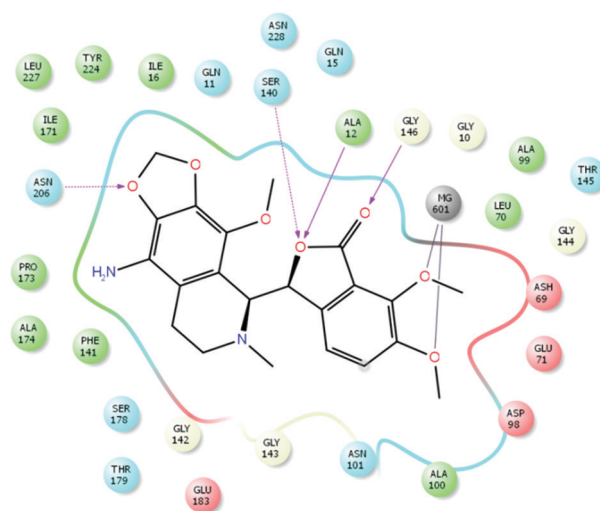


Figure 4: Amino-acid residue interactions exhibited by the molecule amino-Noscapine in the active site of the target PDB-3E22.

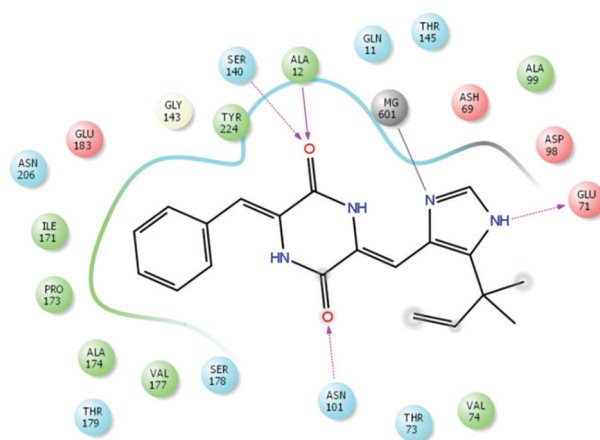


Figure 5: Amino-acid residue interactions exhibited by the molecule (z)-Dehydrophenylahistin in the active site of the target PDB-3E22.

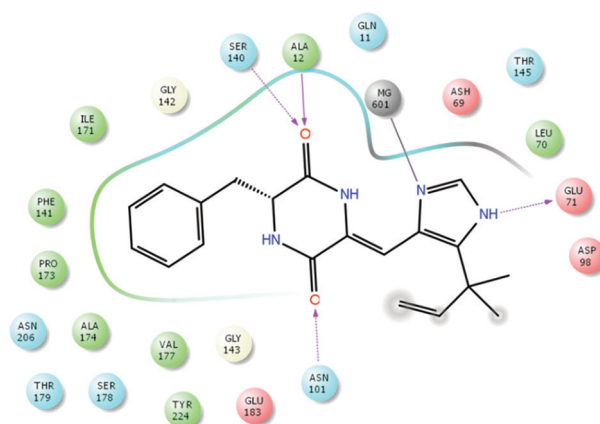


Figure 6: Amino-acid residue interactions exhibited by the molecule (-)-phenylahistin in the active site of the target PDB-3E22.

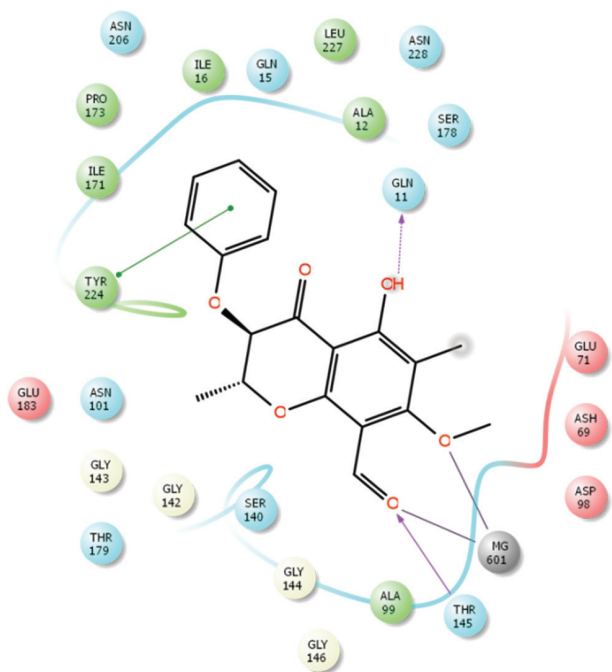


Figure 7: Amino-acid residue interactions exhibited by the molecule Desmosdumotin A in the active site of the target PDB-3E22.

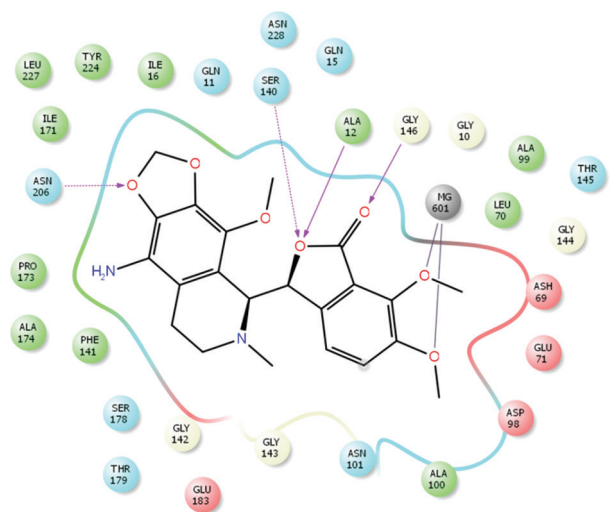


Figure 8: Amino-acid residue interactions exhibited by the molecule amino-Noscapine in the active site of the target PDB-3E22.

ADME properties

Table 3 shows the ADME properties of all the selected tubulin inhibitors. For oral action, no more than two Lipinski rules should be broken. All of the experimental derivatives in this series did not exceed the allowed limit of rule violation. The polar surface area and rotatable bond of all the compounds are within the permitted range of medication similarity qualities.

The QikProp module of Schrodinger programme was used to compute the physicochemical parameters of the

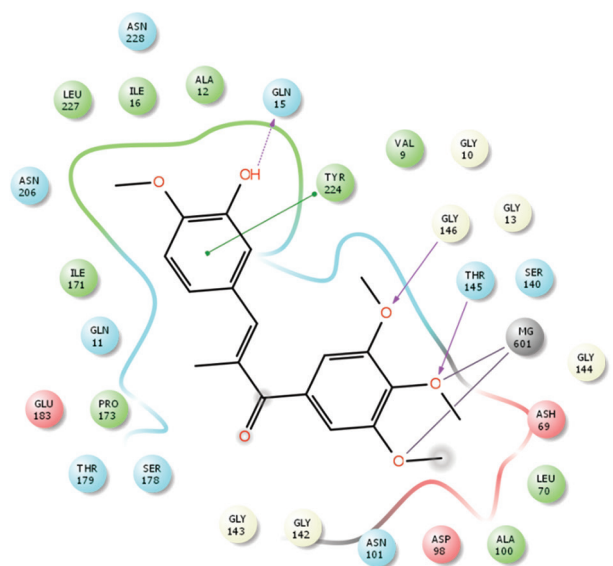


Figure 9: Amino-acid residue interactions exhibited by the molecule Chalcone SD400 in the active site of the target PDB-3E22.

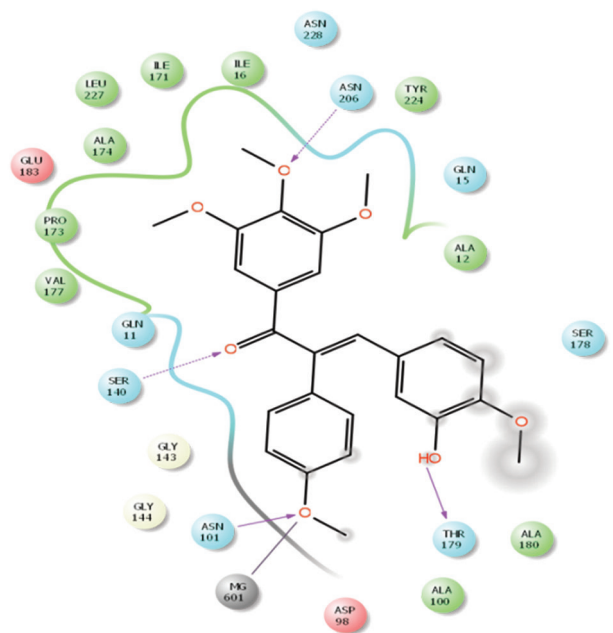


Figure 10: Amino-acid residue interactions exhibited by the molecule alpha-arylchalcone in the active site of the target PDB-3E22.

compounds (1-10). Different *in silico* pharmacokinetic properties of the synthesized compounds was predicted in this study, including polar surface area (PSA), QPlogPo/w, predicted apparent Caco-2 permeability (QPPCaco), predicted brain/blood partition coefficient (QPlogBB), predicted apparent MDCK cell permeability (QPPMDCK), and percent human oral absorption. These pharmacokinetic features were crucial in linking biological activity to physicochemical properties which are displayed in Table 3.

The apparent permeability across the Caco-2 cell membrane is represented by descriptors like QPPCaco. A QPPCaco value of <25 indicated inadequate permeability, whereas a value of >500 indicated superior permeability. All of the inhibitors in the series have good Caco-2 values.

The brain/blood partition coefficient (-4.008 – -0.724) is represented by QPlogBB, and QPPMDCK is the apparent permeability across MDCK cells, which can be used as an excellent non-active transport mimic for the blood brain barrier (BBB). QPlogBB and QPPMDCK values were highest in compound.

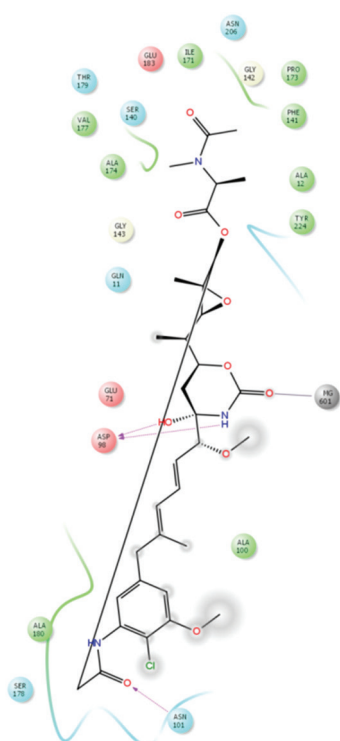


Figure 11: Amino-acid residue interactions exhibited by the molecule Mayatansine in the active site of the target PDB-3E22.

CONCLUSION

In the present study, molecular studies have been performed for finding the potential inhibitor at the CBS of tubulin. After docking these compounds into the CBS, two ligands with the lowest binding free energy and the best forms of interaction with the CBS were chosen. Furthermore, high-throughput virtual screening, SP, XP, and methodologies were performed. Results revealed that compound Centaureldin and Chalcones MDL showed the highest docking scores of -7.76 and -6.21 kcal/mol, respectively, when compared with the cocrystal ligands of PDB-3E22. Post-MM-GBSA analysis of these potent inhibitors showed dG binding values -37.83 and -28.37 kcal/mol, respectively. On the basis of final screened compounds, we can further develop pharmacophore model and screened potential compounds against tubulin protein.

ACKNOWLEDGMENT

I am profoundly grateful to ISF College of Pharmacy, Moga for providing research facilities.

REFERENCES

1. Sheng L, Hao SL, Yang WX, Sun Y. The multiple functions of kinesin-4 family motor protein KIF4 and its clinical potential. *Gene* 2018;678:90-9.
2. Bates D, Eastman A. Microtubule destabilising agents: Far more than just antimetabolic anticancer drugs. *Br J Clin Pharmacol* 2017;83:255-68.
3. Jordan MA, Wilson L. Microtubules as a target for anticancer drugs. *Nat Rev Cancer* 2004;4:253-65.
4. Khattab M, Al-Karmalawy A. Computational repurposing of benzimidazole anthelmintic drugs as potential colchicine binding site inhibitors. *Future Med Chem* 2021;13:1623-38.
5. Mukhtar E, Adhami VM, Mukhtar H. Targeting

Table 3: ADME properties predictions of ligands

S. No.	Compounds Name	QP log Po/w ¹	QPP Caco ²	QP logBB ³	QPPMDCK ⁴	#metab	QP logKhsa ⁵	Percent human oral absorption ⁶
1	Centaureldin	0.855	191.326	-1.411	82.801	10	-0.447	72.789
2	Chalcones MDL	2.471	762.65	-0.918	369.112	1	-0.1	93.001
3	(-)- phenylahistin	2.643	462.031	-1.078	214.733	2	0.101	90.114
4	(Z)- Dehydrophenylahistin	2.726	409.63	-1.267	188.535	0	0.112	89.665
5	alpha- arylchalcone	4.977	2226.666	-0.8	1175.233	6	0.597	100
6	Chalcone SD400	3.716	1877.631	-0.737	977.44	6	0.221	100
7	Mayatansinol	2.95	438.313	-1.49	330.152	9	-0.208	78.544
8	Noscapine	2.034	822.261	0.317	442.961	7	-0.408	91.03

¹Predicted octanol/water partition coefficient (Range= -2.0 – 6.5), ²Predicted apparent Caco-2 cell permeability in nm/sec. Caco-2 cells are a model for the gut blood barrier (<25% is poor, >500 great), ³predicted brain/blood partition coefficient, ⁴Predicting apparent passive permeability of Caco-2 and MDCK cell, ⁵Human serum albumin binding, ⁶Percent human oral absorption on 0–100% scale. >80% is high, <25% is poor

- microtubules by natural agents for cancer therapy. *Mol Cancer Ther* 2014;13:275-84.
- Wu X, Wang Q, Li W. Recent advances in heterocyclic tubulin inhibitors targeting the colchicine binding site. *Anticancer Agents Med Chem* 2016;16:1325-38.
 - Brenner DR, Weir HK, Demers AA, Ellison LF, Louzado C, Shaw A, *et al.* Projected estimates of cancer in Canada in 2020. *CMAJ* 2020;192:E199-205.
 - Shim JS, Liu JO. Recent advances in drug repositioning for the discovery of new anticancer drugs. *Int J Biol Sci* 2014;10:654-63.
 - Parvathaneni V, Kulkarni NS, Muth A, Gupta V. Drug repurposing: A promising tool to accelerate the drug discovery process. *Drug Discov Today* 2019;24:2076-85.
 - Abdullahi M, Adeniji SE. *In-silico* molecular docking and ADME/pharmacokinetic prediction studies of some novel carboxamide derivatives as anti-tubercular agents. *Chem Afr* 2020;3:989-1000.
 - Anant A, Ali A, Ali A, Gupta GD. A Computational approach to discover potential quinazoline derivatives against CDK4/6 kinase. *J Mol Struct* 2021;1245:131079.
 - Simon L, Imane A, Srinivasan KK, Pathak L, Daoud I. *In silico* drug-designing studies on flavanoids as anticancer agents: Pharmacophore mapping, molecular docking, and Monte Carlo method-based QSAR modeling. *Interdiscip Sci* 2017;9:445-58.
 - Arooj M, Sakkiah S, Kim S, Arulalapperumal V, Lee KW. A combination of receptor-based pharmacophore modeling & QM techniques for identification of human chymase inhibitors. *PLoS One* 2013;8:e63030.
 - Anand SA, Chandrasekaran L, Kuppusamy S, Kabilan S. Comparison of molecular docking and molecular dynamics simulations of 1, 3-thiazin-4-one with MDM2 protein. *Int Lett Chem Phys Astron* 2015;60:161-7.
 - Chen H, Lyne PD, Giordanetto F, Lovell T, Li J. On evaluating molecular-docking methods for pose prediction and enrichment factors. *J Chem Inf Model* 2006;46:401-15.
 - Elokely KM, Doerksen RJ. Docking challenge: Protein sampling and molecular docking performance. *J Chem Inf Model* 2013;53:1934-45.
 - Bode W, Turk D, Karshikov A. The refined 1.9-Å X-ray crystal structure of D-Phe-Pro-Arg chloromethylketone-inhibited human α -thrombin: Structure analysis, overall structure, electrostatic properties, detailed active-site geometry, and structure-function relationships. *Protein Sci* 1992;1:426-71.
 - Tripathi SK, Singh SK, Singh P, Chellaperumal P, Reddy KK, Selvaraj S. Exploring the selectivity of a ligand complex with CDK2/CDK1: A molecular dynamics simulation approach. *J Mol Recognit* 2012;25:504-12.
 - Stanzione F, Giangreco I, Cole JC. Use of molecular docking computational tools in drug discovery. *Prog Med Chem* 2021;60:273-343.
 - Sottriffer C, Klebe G. Identification and mapping of small-molecule binding sites in proteins: Computational tools for structure-based drug design. *Farmacologia* 2002;57:243-51.
 - Hu X, Li H. Force spectroscopy studies on protein-ligand interactions: A single protein mechanics perspective. *FEBS Lett* 2014;588:3613-20.
 - Tran-Nguyen VK, Bret G, Rognan D. True accuracy of fast scoring functions to predict high-throughput screening data from docking poses: The simpler the better. *J Chem Inf Model* 2021;61:2788-97.
 - Morris GM, Lim-Wilby M. Molecular docking. *Methods Mol Biol* 2008;443:365-82.
 - Kirchmair J, Markt P, Distinto S, Schuster D, Spitzer GM, Liedl KR, *et al.* The protein data bank (PDB), its related services and software tools as key components for *in silico* guided drug discovery. *J Med Chem* 2008;51:7021-40.
 - Totrov M, Abagyan R. Flexible ligand docking to multiple receptor conformations: A practical alternative. *Curr Opin Struct Biol* 2008;18:178-84.
 - Huang SY, Zou X. Advances and challenges in protein-ligand docking. *Int J Mol Sci* 2010;11:3016-34.
 - Hou T, Wang J, Li Y, Wang W. Assessing the performance of the MM/PBSA and MM/GBSA methods. 1. The accuracy of binding free energy calculations based on molecular dynamics simulations. *J Chem Inf Model* 2011;51:69-82.
 - Li J, Abel R, Zhu K, Cao Y, Zhao S, Friesner RA. The VSGB 2.0 model: A next generation energy model for high resolution protein structure modeling. *Proteins* 2011;79:2794-812.
 - Kumar BK, Faheem, Sekhar KV, Ojha R, Prajapati VK, Pai A, *et al.* Pharmacophore based virtual screening, molecular docking, molecular dynamics and MM-GBSA approach for identification of prospective SARS-CoV-2 inhibitor from natural product databases. *J Biomol Struct Dyn* 2022;40:1363-86.
 - Prasanthi GJ. *In-silico* estimation on oral bioavailability and drug-likeness of mono and bis-mannich bases of piperazine derivatives. *J Glob Trends Pharm Sci* 2014;5:1485-8.
 - Asati V, Bharti SK. Design, synthesis and molecular modeling studies of novel thiazolidine-2, 4-dione derivatives as potential anti-cancer agents. *J Mol Struct* 2018;1154:406-17.
 - Tantawy MA, Shaheen S, Kattan SW, Alelwani W, Barnawi IO, Elmgeed GA, *et al.* Cytotoxicity, *in silico* predictions and molecular studies for androstane heterocycle compounds revealed potential antitumor agent against lung cancer cells. *J Biomol Struct Dyn* 2020;40:1-14.